

Individual mapping of innate immune cell activation is a candidate marker of patient-specific trajectories of disability worsening in Multiple Sclerosis

Benedetta Bodini^{1,2*}, Emilie Poirion^{1*}, Matteo Tonietto¹, Charline Benoit¹, Raffaele Palladino^{3,4}, Elisabeth Maillart^{1,2}, Erika Portera¹, Marco Battaglini⁵, Geraldine Bera^{1,2}, Bertrand Kuhnast⁶, Céline Louapre^{1,2}, Michel Bottlaender⁶, and Bruno Stankoff^{1,2}

* these two authors contributed equally to this work

¹Sorbonne Universités, Institut du Cerveau et de la Moelle épinière, ICM, Hôpital de la Pitié Salpêtrière, Inserm UMR S 1127, CNRS UMR 7225, Paris, France

²Assistance Publique des Hôpitaux de Paris, France

³School of Public Health, Imperial College of London, London, UK

⁴University “Federico II” of Naples, Naples, Italy.

⁵Department of Neurological Sciences, University of Siena, Siena, Italy

⁶CEA, Université Paris Sud, Université Paris-Saclay, Service Hospitalier Frédéric Joliot, Orsay, France

Corresponding author: Bruno Stankoff, MD, PhD

First authors: Benedetta Bodini, Emilie Poirion

Address for correspondence: ICM, Hopital Pitié-Salpêtrière, 47, Bd de l'Hôpital, 75013

Paris, France

Tél. +33(0)157274463

E-mail for correspondence: bruno.stankoff@aphp.fr

E-mails First authors: benedetta.bodini@aphp.fr; emi.poirion@gmail.com

Number of words: 5000

Short running title: Individual maps of innate immunity in MS

ABSTRACT

To develop a novel approach to generate individual maps of white matter (WM) innate immune cell activation using ^{18}F -DPA-714 translocator protein (TSPO) positron emission tomography (PET), and to explore the relationship between these maps and individual trajectories of disability worsening in patients with multiple sclerosis (MS). **Methods:** Patients with MS ($n=37$), whose trajectories of disability worsening over the 2 years preceding study entry were calculated, and healthy controls ($n=19$) underwent magnetic resonance magnetic and ^{18}F -DPA-714 PET. A threshold of significant activation of ^{18}F -DPA-714 binding was calculated with a voxel-wise randomized permutation-based comparison between patients and controls, and used to classify each WM voxel in patients as characterized by a significant activation of innate immune cells (DPA+) or not. Individual maps of innate immune cell activation in the WM were employed to calculate the extent of activation in WM regions-of-interests and to classify each WM lesion as “DPA-active”, “DPA-inactive” or “unclassified”. **Results:** Compared with the WM of healthy controls, patients with MS had a significantly higher percentage of DPA+ voxels in the normal-appearing WM, (NAWM in patients= $24.9\pm 9.7\%$; WM in controls= $14.0\pm 7.8\%$, $p<0.001$). In patients with MS, the percentage of DPA+ voxels showed a significant increase from NAWM, to perilesional areas, T2 hyperintense lesions and T1 hypointense lesions ($38.1\pm 13.5\%$, $45.0\pm 17.9\%$, and $51.9\pm 22.9\%$, respectively, $p<0.001$). Among the 1379 T2 lesions identified, 512 were defined as DPA-active and 258 as DPA-inactive. A higher number of lesions classified as DPA-active (OR=1.13, $p=0.009$), a higher percentage of DPA+ voxels in the NAWM (OR=1.16, $p=0.009$) and in T1-spin-echo lesions (OR=1.06, $p=0.036$), were significantly associated

with a retrospective more severe clinical trajectory in patients with MS. **Conclusion:** A more severe trajectory of disability worsening in MS is associated with an innate immune cells activation inside and around WM lesions. ^{18}F -DPA-714 PET may provide a promising biomarker to identify patients at risk of severe clinical trajectory.

Key words: Multiple Sclerosis, TSPO, Positron Emission Tomography, disability worsening

INTRODUCTION

Multiple sclerosis (MS) is the most frequent demyelinating disease and remains the first cause of non-traumatic neurological disability among young adults (1). During the past decades, great therapeutical progresses have been made in the prevention of clinical relapses. However, the prevention of disability worsening remains a key unsolved issue in the treatment of MS. Disability worsening does not follow homogeneous and stable trajectories over the course of the disease, but instead can be characterized by alternating phases of rapid accrual of disability and clinical stability (2).

The activation of the innate immune system has been shown to play a crucial role in the biological processes contributing to the accrual of clinical disability in MS. Pro-inflammatory innate immune cells are involved in active demyelination and axonal damage, and have the potential to inhibit myelin repair (3). Moreover, white matter (WM) lesions surrounded by a rim of persisting activated microglial cells are found exclusively in post-mortem brains of progressive patients (4). Finally, microglial cells mediate the subpial cortical demyelination associated with meningeal inflammation (5), and their accumulation in both the normal-appearing WM (NAWM) and the grey matter (GM), results in oxydative burst, energy deficit and neurodegeneration (6).

These converging lines of evidence suggest that the activation of the innate immune system acts as a transversal biological mechanism contributing to tissue damage and disability at all stages of the disease.

The most popular imaging tool to measure innate immune cells is positron emission tomography (PET) with radiotracers targeting translocator protein (18 kDa) (TSPO), whose expression is upregulated in innate immune cells in the context of inflammatory conditions such as MS (7).

An increased binding of the ^{11}C -PK11195, the first-generation compound developed for TSPO imaging, has been described inside and outside WM lesions, and in the GM of patients with all forms of MS (8,9). Recent studies using ^{11}C -PBR28, a second-generation TSPO tracer, have demonstrated an high binding in the cortex of MS patients (10), and a subject-specific heterogeneity in WM lesions binding (11).

The pyrazolopyrimidine ^{18}F -DPA-714 (12) is a fluorinated second-generation TSPO tracer, which allows a reliable kinetic modelling in humans (13), and a non-invasive quantification through the extraction of reference regions (14,15). In a recent pilot study, ^{18}F -DPA-714 PET could reliably identify focal and diffuse neuroinflammation (16). In this study, we investigated a group of 37 patients with relapsing or progressive MS and a group of healthy controls with ^{18}F -DPA-714 PET. We developed an original post-processing approach to obtain individual maps of innate immune cell activation and to explore the relationship between these individual profiles of innate immune cell activity and patient-specific trajectories of disability worsening in MS.

MATERIALS AND METHODS

Subjects

We recruited 41 patients with MS according to the revised McDonald criteria (17) (13 relapsing-remitting, RR; 15 secondary-progressive, SP; 13 primary-progressive, PP),

and 20 age- and gender-matched healthy controls (HC). Subjects signed written informed consent to participate in a protocol approved by the local ethics committee.

Subjects were genotyped for the rs6971 polymorphism and divided in high- (HABs, 15 MS, 10 HC), mixed- (MABs, 22 MS, 9 HC), and low-affinity (4 MS, 1 HC) to TSPO binding sites (18). The latter group was excluded from further analysis (Table 1).

Clinical Assessment

At study entry, all patients underwent a neurological examination and were scored using the Expanded Disability Status Scale (EDSS) (19). For each patient, the EDSS score 2 years before study entry was retrospectively collected through the careful revision of primary medical files. Disability worsening over 2 years was evaluated as changes in EDSS between the inclusion visit and 2 years before study entry, and converted into EDSS step change (20).

Patients were classified in untreated, treated with immuno-modulators, or treated with immuno-suppressors according to the main treatment received in the two years preceding study entry (Table 1).

Imaging Acquisition

All subjects underwent a magnetic resonance imaging (MRI) protocol on a Siemens 3T PRISMA scanner, equipped with a 32-channels head coil, and a dynamic ¹⁸F-DPA-714 PET exam on a high-resolution research tomograph within one month from study entry.

MRI protocol included the following sequences: (i) three-dimensional T1-weighted (T1-w) magnetization-prepared rapid gradient-echo (resolution: $1.0 \times 1.0 \times 1.1 \text{ mm}^3$); (ii) T2-weighted image (T2-w, resolution: $0.9 \times 0.9 \times 3.0 \text{ mm}^3$); (iii) three-dimensional fluid-attenuated inversion recovery (FLAIR, resolution: $0.9 \times 0.9 \times 3.0 \text{ mm}^3$) and (iv) pre- and post-gadolinium T1 spin-echo sequences (resolution: $1.0 \times 1.0 \times 3.0 \text{ mm}^3$).

PET protocol consisted of an intravenous bolus injection of $198.4 \pm 22.9 \text{ MBq}$ of ^{18}F -DPA-714 at the beginning of 90 min dynamic acquisition. PET acquisition parameters and image reconstruction are detailed elsewhere (14).

Image Analysis

In patients, T2 hyperintense lesions were manually contoured on T2-w scans with reference to FLAIR images. T1 hypointense (T1-se) and gadolinium enhancing (Gd+) lesions were respectively contoured on pre- and post-gadolinium T1 spin-echo sequences. The corresponding lesion masks were generated and aligned to the individual T1-w scan using FLIRT (FSL, v5.0.9). After “lesion-filling” in patients only (21), T1-w scans were segmented using FreeSurfer, v6.0.

The following regions of interest (ROIs) were then defined in patients: (i) NAWM, defined as the WM outside visible lesions on T2-w scans; (ii) perilesional area, defined as the 2-voxel rim outside lesion border; (iii) T2 lesions; (iv) T1-se lesions and (v) Gd+ lesions. In healthy controls, the WM ROI was defined.

In each subject, T1-w were non-linearly registered onto a standard brain image (MNI) using a combination of affine and symmetric diffeomorphic transformations

calculated with ANTs, v2.2. The derived transforms were used to align all the previously generated ROIs to standard space.

Voxel-wise ^{18}F -DPA-714 distribution volume ratio (DVR) parametric maps were calculated using the Logan graphical method based on reference region, extracted using a supervised clustering algorithm (Supplemental Fig. 1) (14). DVR maps were co-registered to the T1-w images with FLIRT and normalized to MNI using the previously derived transformations.

Generation of Individual Maps of Activated Microglia

The objective of this part of the analysis was to determine for each individual DVR map, which voxels were characterized by a significant activation of innate immune cells (hereinafter referred to as DPA+ voxels). The method we developed involves two steps: the definition of a threshold (Fig. 1A) and the classification of voxels (Fig. 1B).

For the threshold definition, we initially identified WM regions of significant group differences between the DVR maps of patients with MS and HCs. This was done by performing a voxel-wise non-parametric permutation-based t-test with threshold-free cluster enhancement using RANDOMISE from FSL, where age, gender, and TSPO affinity were included as covariates. From these regions of significant difference, we extracted the mean DVR in patients ($\overline{\text{DVR}}_{\text{MS}}$) and healthy controls ($\overline{\text{DVR}}_{\text{HC}}$), which were used to calculate a relative percentage threshold as: $100 \cdot \frac{\overline{\text{DVR}}_{\text{MS}} - \overline{\text{DVR}}_{\text{HC}}}{\overline{\text{DVR}}_{\text{HC}}}$.

The second step, the voxel classification, was performed in MNI space for each subject separately. Here we classified as DPA+ all those voxels whose DVR value exceeded the mean DVR value of the healthy control voxels in the same MNI position of

more than the previously calculated percentage threshold. This resulted in individual maps of microglia activation, consisting of binary masks of DPA+ voxels.

Given the impact of the TSPO affinity on the DVR estimates, all the aforementioned steps after the randomize analysis (threshold calculation and voxels classification) were performed separately for HABs and MABs.

The percentage of DPA+ voxels over total volume in the NAWM, perilesional area, T2 lesions, T1-se lesions and Gd+ lesions of patients with MS, and in the WM of HCs, was then calculated.

Single Lesion Classification

In patients, to minimize partial volume effect, only WM lesions with a volume greater than 50 voxels were analyzed. Each lesion was then classified as (i) DPA-active (percentage of DPA+ voxels over lesion volume $\geq 50\%$); (ii) DPA-inactive (percentage of DPA+ voxels over lesion volume $\leq 10\%$) and (iii) unclassified (lesion not falling into one of the abovementioned classes).

Statistical Analysis

Linear regression models were used to assess unadjusted differences in: (i) age between HC and MS subgroups (RR, SP and PP); (ii) disease duration, T2 lesion load, and T1-se lesion load between MS subgroups. Fisher exact tests were used to determine whether there were significant differences in the distribution of: (i) gender and TSPO affinity between HC and MS subgroups; (ii) treatment among MS subgroups. Ordered logistic regression models were used to test differences in EDSS and EDSS step change among MS subgroups.

A multiple linear regression model including age, gender and TSPO affinity as covariates, was employed to assess the difference in mean DVR (response variable) between the NAWM of the whole group of MS patients and the WM of HC (predictors).

In MS patients only, a linear-mixed regression model, accounting for the hierarchical structure of the data, was employed to assess the difference in mean DVR (response variable) between ROIs (NAWM, perilesional area, T2 lesions, and T1-se lesions, as predictors). Age, gender, MS subgroup, TSPO affinity and treatment type were included as covariates. Subjects were included in the model as random effect while ROIs and the other covariates were assumed as fixed in the population.

A similar approach was performed to test i) the difference in percentage of DPA+ voxels (response variable) between the NAWM of MS patients and the WM of HC (predictors), and ii) the difference in percentage of DPA+ voxels (response variable) between ROIs (predictors).

In MS patients only, two linear regression models were employed to assess differences between MS subgroups (predictors) in the number of DPA-active/inactive lesions (response variable), respectively. Age, gender, treatment type and total number of T2 lesions were included as covariates.

Multiple ordered logistic regression models were employed to assess which parameters were associated with EDSS at study entry or with EDSS step change over the 2 years preceding study entry (response variable). The following parameters were considered (predictors): (i) T2 lesion load; (ii) T1-se lesion load; (iii) number of T2

lesions; percentage of DPA+ voxels in (iv) NAWM, (v) perilesional area, (vi) T2 lesions and (vii) T1-se lesions; number of (viii) DPA-active and (ix) DPA-inactive lesions. Age, gender, MS subgroup, and treatment type were included as covariates of no interest.

Statistical analyses were performed in Stata (v14.0 MP). Demographic data are presented as mean±standard deviation (SD), while EDSS and EDSS step change are presented as median[range]. For inferential statistics, results are reported as estimated marginal mean±standard error (SE) or median[interquartile range IQR], except otherwise specified. For all tests, the level of statistical significance was set at p-value<0.05, and Bonferroni corrected pairwise comparisons of the estimated marginal means were performed when necessary.

RESULTS

Demographic, Clinical and MRI Variables

Subject's demographics, TSPO genotype, clinical and radiological data are reported in Table 1. No significant difference was found between HCs and MS subgroups for age ($p=0.27$), gender ($p=0.56$) and TSPO affinity ($p=0.85$). Disease duration, EDSS and treatment type were significantly different between MS subgroups (respectively, $p=0.0018$, $p=0.001$, $p=0.001$). EDSS step change, T2 and T1-se lesion load were not statistically different between MS subgroups (respectively, $p=0.84$, $p=0.58$, $p=0.39$).

An Increasing Gradient of Innate Immune Cells Activation From Normal-appearing White Matter to MS Lesions

In WM areas of significant differences between patients and HCs, the mean DVR values were 0.92 ± 0.09 and 0.99 ± 0.09 in patients with MS (HAB and MAB respectively), and 0.77 ± 0.06 and 0.84 ± 0.07 in HCs (HAB and MAB respectively). Thus, the relative changes between groups were 19.34% and 17.29% for HAB and MAB respectively. A final relative group difference rounded to 20% was retained for both HAB and MAB, and used as a threshold to identify DPA+ voxels. As a result, for each subject an individual map of innate immune cell activation was generated (Fig. 2).

The mean DVR in the NAWM of patients with MS was significantly higher (mean \pm SE= 0.94 ± 0.01 , $p=0.002$) than the DVR in the WM of healthy controls (0.87 ± 0.02), (Fig. 3A). In patients with MS, the mean DVR was statistically different

among ROIs ($p=0.002$) (Supplemental Table 1), with an increase from NAWM, to perilesional area (1.03 ± 0.02), T2 lesions (1.01 ± 0.02) and T1-se lesions (1.05 ± 0.02).

The percentage of DPA+ voxels in the NAWM of patients with MS was significantly higher ($24.6\pm 1.4\%$, $p<0.001$) than the percentage of DPA+ voxels in the WM of healthy controls ($14.6\pm 2.0\%$), (Fig. 3B). In patients with MS, the percentage of DPA+ voxels was statistically different among ROIs ($p<0.001$) (Supplemental Table 1), with a significant increase from NAWM, to perilesional area ($38.1\pm 2.6\%$), T2 lesions ($45.0\pm 2.6\%$) and T1-se lesions ($51.8\pm 2.6\%$).

Active MS Lesions Are Unmasked by ^{18}F -DPA-714 PET

In MS patients, a total number of 1379 T2 lesions were analyzed (median[IQR]: RR=32[26]; PP=29[23.5]; SP=32[34]). Among the considered lesions, 176 (12.8%) were also identified as T1-se lesions. Only 3 Gd+ lesions were identified based on post-gadolinium T1 spin-echo sequence.

Based on ^{18}F -DPA-714 PET, 512 (37.1%) of total lesions were defined as DPA-active (RR=13[6]; PP=8[11]; SP=14[16]), and 258 (18.7%) as DPA-inactive (RR=6[7]; PP=5[5.5]; SP=7.5[6]) (Fig. 4). No statistical difference was found in the number of DPA-active/inactive lesions among MS subgroups (Supplemental Table 2).

Disability Trajectories correlate with individual Patterns of Innate Immune Cells Activation

A more severe trajectory of disability worsening, as measured by a greater 2-year EDSS step change, was significantly associated with each of the following parameters: percentage of DPA+ voxels in the NAWM (OR: 1.16, $p=0.009$); percentage of DPA+ voxels in T1-se lesions (OR: 1.06, $p=0.036$); and number of DPA-active lesions (OR: 1.13, $p=0.009$). None of the MR/PET imaging parameters considered was significantly associated with the EDSS level at study entry (Supplemental Table 3).

DISCUSSION

In this study we have developed an original post-processing pipeline of ^{18}F -DPA-714 PET images to obtain individual maps of innate immune cell activation. We showed that patients with MS are characterized by an increased activation of innate immune cells in the WM compared with healthy controls, and we have been able to classify single WM lesions as either DPA-active or DPA-inactive. This novel approach allowed to identify individual profiles of innate immune cells activation, which were shown to correlate with patient-specific trajectories of disability worsening, regardless of the form of the disease.

At the whole-group level, the results of our study confirmed the notion that patients with MS have an increase in microglial/macrophage activation in the WM compared with healthy controls (8,9). In patients we demonstrated an increasing gradient in the percentage of DPA+ voxels from NAWM, to perilesional and lesional WM, with the highest level of activation of innate immune cells being found in WM plaques. Interestingly, the greatest variability in the percentage of DPA+ voxels was found in T1-se hypointense lesions. This finding confirms that a heterogeneous pathological substrate could underlie the hypointense appearance of lesions on T1 spin-echo sequences. While acute lesions could appear as transient hypointensities on T1 spin-echo sequences (22), it is generally considered that T1-se hypointensities in subacute and chronic lesions mostly reflect irreversible tissue damage (23). Our results demonstrate that the content in active innate immune cells of these T1-se hypointensities is largely heterogeneous and often drastically high (24). This finding,

together with the evidence that a higher percentage of DPA+ voxels in hypointense T1-se lesions is associated with a more severe trajectory of disability worsening, suggests that a subset of these T1-se hypointensities could be chronically active and possibly play a key role in disability worsening.

A key finding of this study was the large amount of WM lesions classified as “active” based on ^{18}F -DPA-714 PET (37,1% of T2 lesions), which were completely invisible to Gd+ MRI sequences (only 0.2% of T2 lesions). These results suggest that our original processing of ^{18}F -DPA-714 PET allows to detect sub-acute and chronic active lesions regardless of the form of clinical evolution. It is known that the quantification of WM lesion number and volume has a limited predictive value on disability worsening, especially in progressive MS, which has widely supported the notion that disability progression mostly evolves independently of lesions. Offering the opportunity to move beyond lesion volume and to investigate the biological content of lesions, ^{18}F -DPA-714 PET now allows to revisit the contribution of plaques to disability accrual in MS.

We found that a higher number of DPA-active lesions, and an increased percentage of DPA+ voxels in T1-se hypointense lesions and in the NAWM, were significantly associated with a greater accumulation of clinical disability over 2 years preceding the study entry, regardless of the form of disease. These data indicate that a strong activation of the innate immune system inside WM lesions and in the NAWM, may represent an imaging correlate of an ongoing clinical trajectory characterized by a rapid accumulation of disability in all forms of disease.

Our results are in line with post-mortem studies showing a substantial innate inflammatory activity within lesions throughout the course of the disease (25). Interestingly, in their large post mortem study, Luchetti and colleagues found that a higher proportion of WM lesions with accumulation of HLA+ microglia/macrophages at the lesion border, suggestive of smoldering lesions, was the most relevant predictive marker of disability accrual (25).

Taken together, this post-mortem evidence and our imaging data converge towards the identification of highly activated innate immune cells both in WM lesions and in the NAWM as a key pathophysiological component associated with a severe clinical trajectory in patients with MS. Our *in-vivo* data also raise the hypothesis that, over the course of the disease, a primary activation of innate immune cells inside some WM lesions that does not subsequently resolve can result in a persistent inflammation that predominates at lesion borders, with or without the persistence of active cells inside the lesion (4,26). These subacute inflammatory processes, in turn, may be responsible of a centrifugal innate immune cell activation of the NAWM which, in turn, may drive a cascade of neurotoxic mechanisms including oxidative stress, energy dysregulation, and excitotoxicity (27). This sequence of events may eventually result in the development of neuronal degeneration, spreading from lesions to normal-appearing tissues.

A careful interpretation of our results is required with regard to the suboptimal specificity of TSPO tracers, which are known to bind to active innate immune cells, but also to astrocytes and endothelial cells (15,28). Moreover, in our study we defined a threshold to classify DPA+ voxels, which depends on the same patients to whom it was

then applied, and this might constitute a possible bias. However in order to validate the threshold that identifies DPA+ voxels, we have further applied a leave-one-out approach, repeating 37 times the randomize procedure, each time excluding a different patient from the analysis: we found that this generated identical thresholds to the ones computed in the original permutation-based analysis.

CONCLUSION

Generating *in-vivo* individual maps of innate immune cell activation based on TSPO PET, we demonstrated that the activation of innate immune cells inside WM lesions and in the NAWM is associated with clinical trajectories in patients with MS. TSPO PET has the potential to shed light on the role played by microglia in neurodegeneration. Whether TSPO PET could be used as a biomarker to identify patients likely to enter into a severe clinical trajectory should be confirmed through prospective studies.

DISCLOSURE

Authors have no conflict of interest regarding this article.

ACKNOWLEDGMENTS

We thank the CIC ICM in Paris, the SHFJ CEA, Orsay, the CENIR, and the URC of Pitié Salpêtrière. The study has been funded by ANR grant MNP2008-007125 to BS, and received additional funding from Foundation ARSEP, ECTRIMS, JNLF, FRM. APHP sponsored the Study.

CONTRIBUTION OF AUTHORS

BB, EP, MB and BS contributed to the conception and design of the study. BB, EM, BK, CL, MB, and BS contributed to the acquisition of data. BB, EP, MT, CB, RP, ErP, GB, and BS contributed to the analysis of data. MT, EP and RP performed the statistical analysis. BB, EP, MT and BS wrote the manuscript.

KEY POINTS

QUESTION: Do individual maps of innate immune cell activation generated from ^{18}F -DPA-714 TSPO PET reflect trajectories of disability worsening in patients with MS?

PERTINENT FINDINGS: individual maps of innate immune cell activation generated from dynamic ^{18}F -DPA-714 PET in a cohort of 37 patients with MS showed a gradient of binding increase from the normal-appearing white matter to white matter lesions. The number of lesions characterized by innate immune cell activation and the extent of activation in the normal-appearing white matter were significantly associated with a more severe clinical trajectory in patients with MS.

IMPLICATIONS FOR PATIENT CARE: Individual mapping of ^{18}F -DPA-714 PET may provide a promising imaging biomarker to identify patients at risk to enter into a severe clinical phase of the disease course.

REFERENCES

1. Reich DS, Lucchinetti CF, Calabresi PA. Multiple sclerosis. *N Engl J Med*. 2018;378:169-180.
2. Confavreux C, Vukusic S, Moreau T, Adeleine P. Relapses and progression of disability in multiple sclerosis. *N Engl J Med*. 2000;343:1430-1438.
3. Peferoen LAN, Vogel DYS, Ummenthum K, et al. Activation status of human microglia is dependent on lesion formation stage and remyelination in multiple sclerosis. *J Neuropathol Exp Neurol*. 2015;74:48-63.
4. Frischer JM, Weigand SD, Guo Y, et al. Clinical and pathological insights into the dynamic nature of the white matter multiple sclerosis plaque. *Ann Neurol*. 2015;78:710-721.
5. Howell OW, Reeves CA, Nicholas R, et al. Meningeal inflammation is widespread and linked to cortical pathology in multiple sclerosis. *Brain*. 2011;134:2755-2771.
6. Fischer MT, Sharma R, Lim JL, et al. NADPH oxidase expression in active multiple sclerosis lesions in relation to oxidative tissue damage and mitochondrial injury. *Brain*. 2012;135:886-899.
7. Banati RB, Newcombe J, Gunn RN, et al. The peripheral benzodiazepine binding site in the brain in multiple sclerosis. *Brain*. 2000;123:2321-2337.
8. Giannetti P, Politis M, Su P, et al. Increased PK11195-PET binding in normal-appearing white matter in clinically isolated syndrome. *Brain*. 2015;138:110-119.
9. Rissanen E, Tuisku J, Rokka J, et al. In vivo detection of diffuse inflammation in secondary progressive multiple sclerosis using PET imaging and the radioligand ¹¹C-PK11195. *J Nucl Med*. 2014;55:939-944.
10. Herranz E, Gianni C, Louapre C, et al. Neuroinflammatory component of gray matter pathology in multiple sclerosis. *Ann Neurol*. 2016;80:776-790.
11. Datta G, Colasanti A, Kalk N, et al. ¹¹C-PBR28 and ¹⁸F-PBR111 detect white matter inflammatory heterogeneity in multiple sclerosis. *J Nucl Med*. 2017;58:1477-1482.
12. James ML, Fulton RR, Vercoullie J, et al. DPA-714, a new translocator protein-specific ligand: synthesis, radiofluorination, and pharmacologic characterization. *J*

Nucl Med. 2008;49:814-822.

13. Lavisse S, García-Lorenzo D, Peyronneau M-AM-AA, et al. Optimized quantification of translocator protein radioligand 18F-DPA-714 uptake in the brain of genotyped healthy volunteers. *J Nucl Med.* 2015;56:1048-1054.
14. García-Lorenzo D, Lavisse S, Leroy C, et al. Validation of an automatic reference region extraction for the quantification of [18F]DPA-714 in dynamic brain PET studies. *J Cereb Blood Flow Metab.* 2018;38:333-346.
15. Rizzo G, Veronese M, Tonietto M, et al. Generalization of endothelial modelling of TSPO PET imaging: Considerations on tracer affinities. *J Cereb Blood Flow Metab.* 2019;39:874-885.
16. Hagens MHJ, Yaqub M, Golla S V., et al. In vivo assessment of neuroinflammation in progressive multiple sclerosis: a proof of concept study with [18F]DPA714 PET. *J Neuroinflammation.* 2018;15:4-13.
17. Polman CH, Reingold SC, Edan G, et al. Diagnostic criteria for multiple sclerosis: 2005 revisions to the “McDonald Criteria.” *Ann Neurol.* 2005;58:840-846.
18. Owen DR, Yeo AJ, Gunn RN, et al. An 18-kDa translocator protein (TSPO) polymorphism explains differences in binding affinity of the PET radioligand PBR28. *J Cereb Blood Flow Metab.* 2012;32:1-5.
19. Kurtzke JF. Rating neurologic impairment in multiple sclerosis: an expanded disability status scale (EDSS). *Neurology.* 1983;33:1444-1452.
20. Weinshenker BG, Issa M, Baskerville J. Meta-analysis of the placebo-treated groups in clinical trials of progressive MS. *Neurology.* 1996;46:1613-1619.
21. Chard DT, Jackson JS, Miller DH, Wheeler-Kingshott CAM. Reducing the impact of white matter lesions on automated measures of brain gray and white matter volumes. *J Magn Reson Imaging.* 2010;32:223-228.
22. van Waesberghe JH, van Walderveen MA, Castelijns JA, et al. Patterns of lesion development in multiple sclerosis: longitudinal observations with T1-weighted spin-echo and magnetization transfer MR. *AJNR Am J Neuroradiol.* 1998;19:675-83.
23. Sahraian MA, Radue E-W, Haller S, Kappos L. Black holes in multiple sclerosis: definition, evolution, and clinical correlations. *Acta Neurol Scand.* 2009;122:1-8.
24. Giannetti P, Politis M, Su P, et al. Microglia activation in multiple sclerosis black

holes predicts outcome in progressive patients: An in vivo [(11)C](R)-PK11195-PET pilot study. *Neurobiol Dis.* 2014;65:203-210.

25. Luchetti S, Fransen NL, van Eden CG, Ramaglia V, Mason M, Huitinga I. Progressive multiple sclerosis patients show substantial lesion activity that correlates with clinical disease severity and sex: a retrospective autopsy cohort analysis. *Acta Neuropathol.* 2018;135:511-528.
26. Prineas JW, Kwon EE, Cho E-S, et al. Immunopathology of secondary-progressive multiple sclerosis. *Ann Neurol.* 2001;50:646-657.
27. Mahad DH, Trapp BD, Lassmann H. Pathological mechanisms in progressive multiple sclerosis. *Lancet Neurol.* 2015;14:183-193.
28. Nutma E, Stephenson JA, Gorter RP, et al. A quantitative neuropathological assessment of translocator protein expression in multiple sclerosis. *Brain,* 2019; 142:3440-3455.

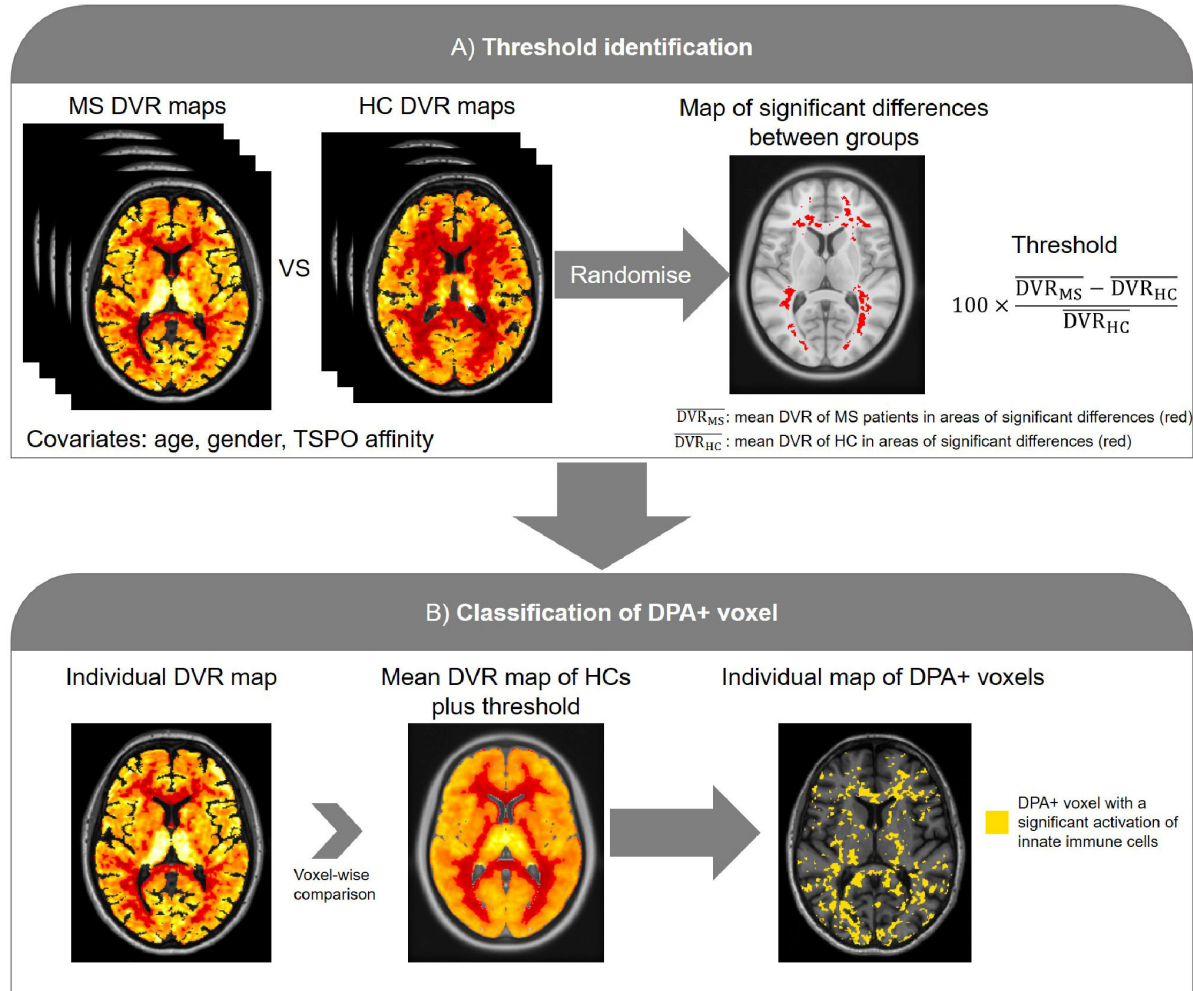


Figure 1: Flowchart of the image analysis pipeline applied to generate individual maps of innate immune cell activation, based on ^{18}F -DPA-714 PET.

Panel A): definition of a threshold to identify innate immune cell activation. Regions of significant group differences between the distribution volume ratio (DVR) maps of patients with MS and healthy controls (HC) were identified through a voxel-wise non-parametric permutation-based t-test. From these regions of significant difference, the mean DVR in patients and HCs were extracted and used to calculate a relative percentage threshold.

Panel B): Classification of DPA+ voxels. All those voxels whose DVR value exceeded the mean DVR value of the HC voxels in the same MNI position of more than the previously calculated percentage threshold were classified as DPA+ voxels.

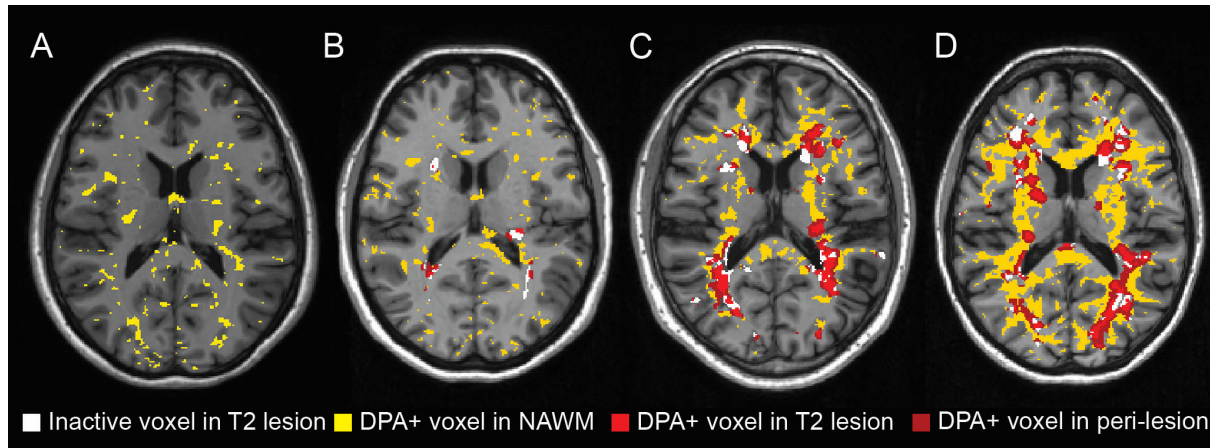


Figure 2: Individual maps of immune cell activation

Individual maps of innate immune cell activation in a single healthy control (A), and in 3 patients with MS characterized by a sparse (B), intermediate (C) and extensive (D) innate immune cell activation. Lesional inactive voxels in patients are represented in white, while voxels characterized by a significant activation of innate immune cells are displayed in yellow in normal-appearing white matter (NAWM), in dark red in perilesional areas, and in light red inside T2 lesions.

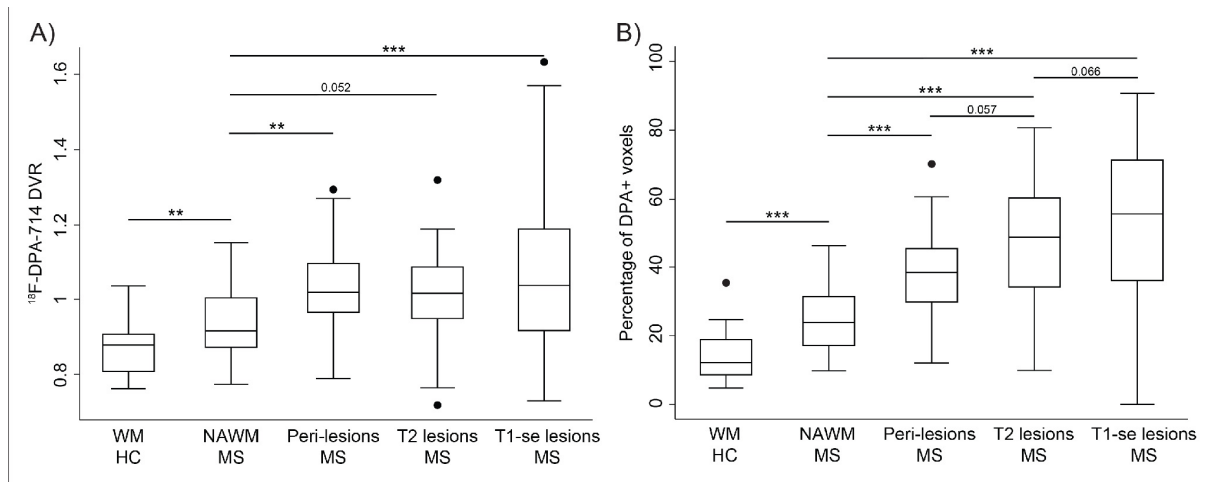


Figure 3: A gradient of innate immune cells activation from normal white matter to MS lesions.

Boxplot diagrams showing an increasing mean distribution volume ratio (DVR, panel A) and percentage of voxels classified as activated (DPA+, panel B), from the white matter (WM) of healthy controls (HC) and the normal-appearing WM (NAWM) of patients with MS, to MS lesions. **: $p < 0.01$, ***: $p < 0.001$

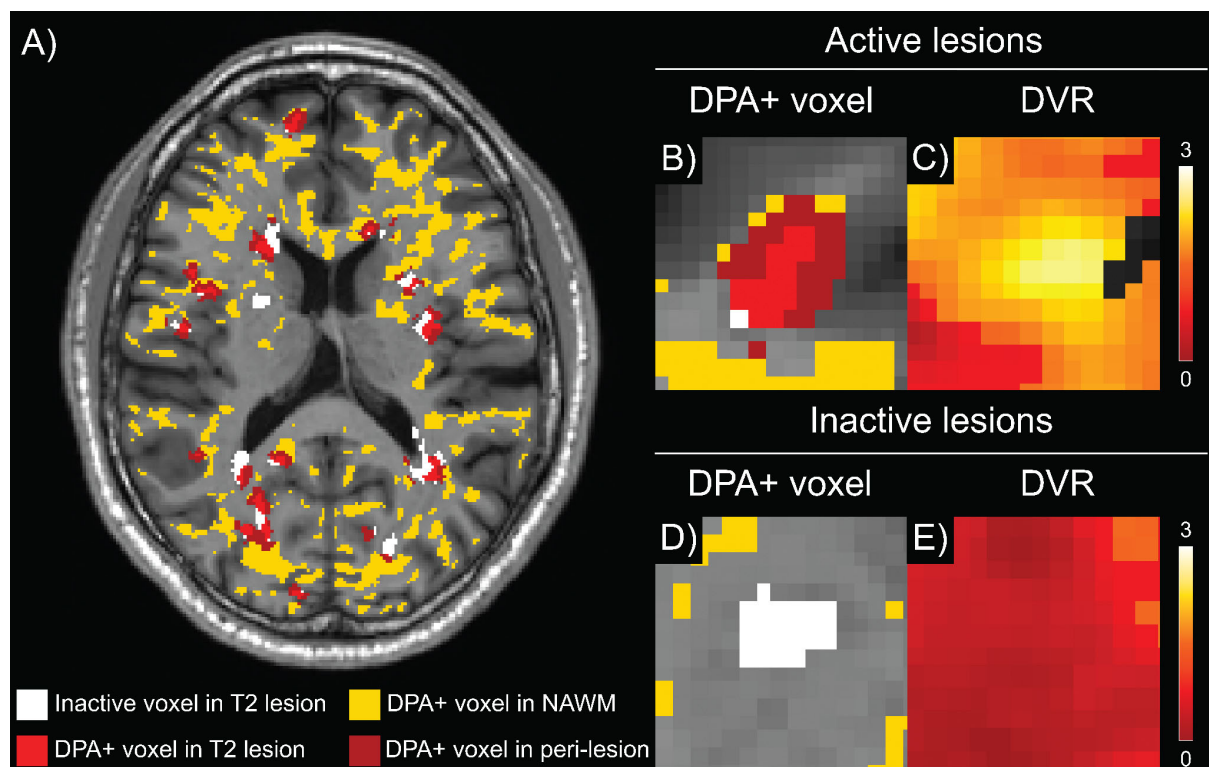


Figure 4: Classification of white matter lesions based on innate immune cell activation

A map of innate immune cell activation in a single patient is shown in A: lesional inactive voxels are displayed in white, while voxels characterized by a significant activation of innate immune cells (DPA+) are displayed in yellow in the normal-appearing white matter, in dark red in perilesional areas, and in light red inside lesions. A single T2 lesion classified as DPA-active is displayed in B, with the corresponding distribution volume ratio (DVR) map, displayed in C. An example of a T2 lesion with an inactive center and an inactive perilesional area is represented in D, and its corresponding DVR map is displayed in E.

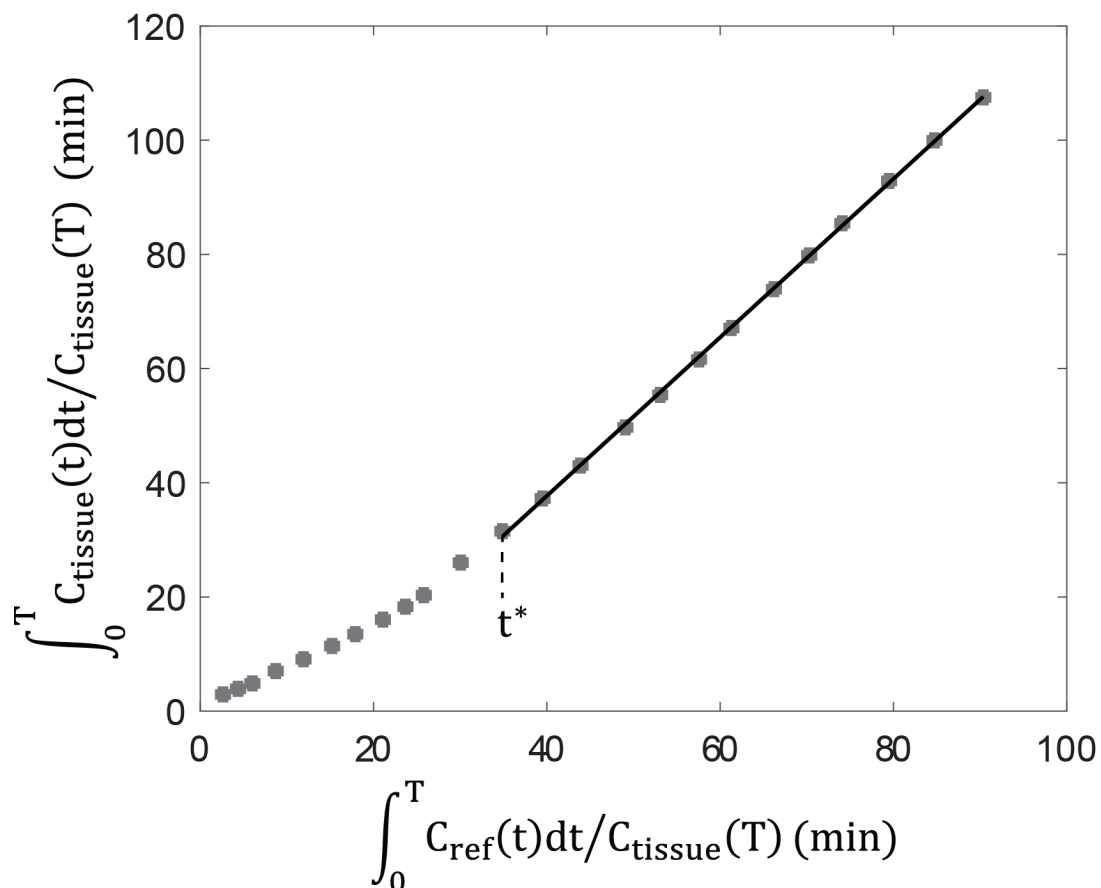
TABLE

Table 1: Demographic, clinical and radiological characteristics of patients and healthy controls

Demographic, clinical and radiological characteristics	Healthy controls	Relapsing-remitting patients	Secondary-progressive patients	Primary-progressive patients
Number	19	11	14	12
Age (years) mean \pm SD	46.6 \pm 14.3	42.6 \pm 13.3	52.4 \pm 9.3	47.0 \pm 10.3
Gender, female/male	13/6	8/3	10/4	3/9
Genotype (MAB/HAB)	10/9	4/7	5/9	6/6
Disease duration (years) mean \pm SD	-	6.7 \pm 4.4	12.9 \pm 6.0	6.7 \pm 2.9
EDSS, median[range]	-	3.5 [2-6]	6 [3.5-7.5]	6 [3-7.5]
EDSS step change, median[range]	-	1 [0-2.5]	1 [0-4.5]	1 [0-2]
T2 lesion load, cc, mean \pm SD	-	11.1 \pm 7.3	14.6 \pm 8.7	16.0 \pm 16.4
BH lesion load, cc, mean \pm SD	-	1.0 \pm 1.2	3.0 \pm 3.2	2.8 \pm 5.5
Disease Modifying Treatment (untreated/immunosuppressor)	-	1/5/5	7/2/5	11/0/1

SUPPLEMENTAL MATERIALS

Supplemental Figure 1



Logan plot with reference region in the normal appearing white matter of a representative patient with multiple sclerosis. The DVR is estimated from the following equation: $\int_0^T C_{tissue}(t)dt/C_{tissue}(T) = DVR \cdot \int_0^T C_{ref}(t)dt/C_{tissue}(T) + const$, where $C_{tissue}(t)$ is the activity concentration in the voxel under analysis and $C_{ref}(t)$ is the activity concentration in the reference region extracted using a supervised clustering algorithm. The linear fit (black line) was obtained after an equilibration time of $t^* = 27.5$ min.

Supplemental Table 1

Difference in mean ¹⁸F-DPA-714 DVR values and percentages of DPA+ voxels between ROIs (NAWM, perilesional area, T2 lesions, and T1-se lesions).

18F-DPA-714 DVR						
test	Coef.	SE	t	p	95% CI	
NAWM in MS vs WM in HC	0.07	0.02	3.35	0.002	0.03	0.11
test	Coef.	SE	z	p (bonf)	95% CI	
PERI in MS vs NAWM in MS	0.09	0.03	3.60	0.002	0.03	0.16
LES in MS vs NAWM in MS	0.07	0.03	2.63	0.052	-0.00	0.14
BH in MS vs NAWM in MS	0.11	0.03	4.19	0.000	0.04	0.19
LES in MS vs PERI in MS	-0.03	0.03	-0.97	1.000	-0.10	0.04
BH in MS vs PERI in MS	0.02	0.03	0.71	1.000	-0.05	0.09
BH in MS vs LES in MS	0.05	0.03	1.65	0.595	-0.03	0.12
Percentage of DPA+ voxel						
test	Coef.	SE	t	p	95% CI	
NAWM in MS vs WM in HC	9.96	2.47	4.03	0.000	5.00	14.92
test	Coef.	SE	z	p (bonf)	95% CI	
PERI in MS vs NAWM in MS	13.24	2.64	5.02	0.000	6.28	20.20
LES in MS vs NAWM in MS	20.08	2.64	7.61	0.000	13.12	27.04
BH in MS vs NAWM in MS	26.90	2.69	10.02	0.000	19.82	33.99
LES in MS vs PERI in MS	6.84	2.64	2.59	0.057	-0.12	13.80
BH in MS vs PERI in MS	13.67	2.69	5.09	0.000	6.58	20.75
BH in MS vs LES in MS	6.83	2.69	2.54	0.066	-0.26	13.91

Supplemental Table 2

Difference in the number of DPA-active/inactive lesions between MS subgroups.

	Predictors	test	Coef.	SE	z	p (bonf)	95% CI	
T2 active	MS subgroups	RR vs PP	3.43	2.16	1.59	0.345	-1.81	8.67
		SP vs PP	4.13	1.76	2.35	0.061	-0.13	8.39
		SP vs RR	0.70	1.77	0.40	1.000	-3.58	4.98
T2 inactive	MS subgroups	RR vs PP	-1.72	1.40	-1.23	0.664	-5.10	1.67
		SP vs PP	0.80	1.13	0.71	1.000	-1.95	3.55
		SP vs RR	2.52	1.14	2.21	0.087	-0.25	5.28

Supplemental Table 3

Associations between parameters of interest and EDSS step change over the 2 years preceding study entry or EDSS at study entry.

	Predictors	Coef.	SE	z	P (bonf)	95% CI	
EDSS step change	T2 lesion load	0.00	0.00	1.20	1.00	0.00	0.00
	T1-se lesion load	0.00	0.00	0.81	1.00	-0.00	0.00
	number of T2 lesions	0.04	0.02	1.91	0.513	-0.00	0.08
	percentage of DPA+ voxels in NAWM	0.15	0.04	3.47	0.009	0.06	0.23
	percentage of DPA+ voxels in perilesional area	0.07	0.03	2.64	0.072	0.02	0.13
	percentage of DPA+ voxels in T2 lesions	0.05	0.02	2.15	0.279	0.00	0.09
	percentage of DPA+ voxels in T1-se lesions	0.06	0.02	2.89	0.036	0.02	0.09
	number of DPA-active lesions	0.12	0.03	3.41	0.009	0.05	0.19
	number of DPA-inactive lesions	-0.22	0.09	-2.59	0.081	-0.39	-0.05
EDSS	T2 lesion load	7.53e-7	2.65e-5	0.03	0.977	-5.11e-5	5.26e-5
	T1-se lesion load	-1.71e-5	8.54e-5	-0.20	0.842	-1.85e-4	1.50e-4
	number of T2 lesions	-0.01	0.02	-0.80	0.424	-0.05	0.02
	percentage of DPA+ voxels in NAWM	-0.03	0.03	-0.78	0.433	-0.09	0.04
	percentage of DPA+ voxels in perilesional area	-0.01	0.02	-0.35	0.726	-0.06	0.04
	percentage of DPA+ voxels in T2 lesions	-0.01	0.02	-0.43	0.664	-0.05	0.03
	percentage of DPA+ voxels in T1-se lesions	0.00	0.01	0.15	0.879	0-.03	0.03
	number of DPA-active lesions	-0.02	0.03	-0.65	0.513	-0.07	0.03
	number of DPA-inactive lesions	-0.03	0.06	-0.56	0.576	-0.15	0.08



The Journal of
NUCLEAR MEDICINE

Individual mapping of innate immune cell activation is a candidate marker of patient-specific trajectories of disability worsening in Multiple Sclerosis

Benedetta Bodini, Emilie Poirion, Matteo Tonietto, Charline Benoit, Raffaele Palladino, Elisabeth Maillart, Erika Portera, Marco Battaglini, Geraldine Bera, Bertrand Kuhnast, Celine Louapre, Michel Bottlaender and Bruno Stankoff

J Nucl Med.

Published online: January 31, 2020.

Doi: 10.2967/jnumed.119.231340

This article and updated information are available at:

<http://jnm.snmjournals.org/content/early/2020/01/16/jnumed.119.231340>

Information about reproducing figures, tables, or other portions of this article can be found online at:

<http://jnm.snmjournals.org/site/misc/permission.xhtml>


Information about subscriptions to JNM can be found at:

<http://jnm.snmjournals.org/site/subscriptions/online.xhtml>

JNM ahead of print articles have been peer reviewed and accepted for publication in *JNM*. They have not been copyedited, nor have they appeared in a print or online issue of the journal. Once the accepted manuscripts appear in the *JNM* ahead of print area, they will be prepared for print and online publication, which includes copyediting, typesetting, proofreading, and author review. This process may lead to differences between the accepted version of the manuscript and the final, published version.

The Journal of Nuclear Medicine is published monthly.
SNMMI | Society of Nuclear Medicine and Molecular Imaging
1850 Samuel Morse Drive, Reston, VA 20190.
(Print ISSN: 0161-5505, Online ISSN: 2159-662X)

© Copyright 2020 SNMMI; all rights reserved.

 SOCIETY OF
NUCLEAR MEDICINE
AND MOLECULAR IMAGING